NEOPLASIA
www.neoplasia.com

Volume 10 Number 8 August 2008 pp. 873–885 873

BH3 Mimetics Reactivate Autophagic Cell Death in Anoxia-Resistant Malignant Glioma Cells[1]

Holger Hetschko*,[2], Valerie Voss*,[2], Christian Senft*, Volker Seifert*, Jochen H.M. Prehn† and Donat Kögel*

*Department of Neurosurgery, Johann Wolfgang Goethe University Clinics, Frankfurt, Germany; †Department of Physiology and Medical Physics and Centre for Human Proteomics, Royal College of Surgeons in Ireland, Dublin 2, Ireland

Abstract

Here, we investigated the specific roles of Bcl-2 family members in anoxia tolerance of malignant glioma. Flow cytometry analysis of cell death in 17 glioma cell lines revealed drastic differences in their sensitivity to oxygen withdrawal (<0.1% O_2). Cell death correlated with mitochondrial depolarization, cytochrome *C* release, and translocation of green fluorescent protein (GFP)–tagged light chain 3 to autophagosomes but occurred in the absence of caspase activation or phosphatidylserine exposure. In both sensitive and tolerant glioma cell lines, anoxia caused a significant up-regulation of BH3-only genes previously implicated in mediating anoxic cell death in other cell types (*BNIP3*, *NIX*, *PUMA*, and *Noxa*). In contrast, we detected a strong correlation between anoxia resistance and high expression levels of antiapoptotic Bcl-2 family proteins Bcl-xL, Bcl-2, and Mcl-1 that function to neutralize the proapoptotic activity of BH3-only proteins. Importantly, inhibition of both Bcl-2 and Bcl-xL with the small-molecule BH3 mimetics HA14-1 and BH3I-2′ and by RNA interference reactivated anoxia-induced autophagic cell death in previously resistant glioma cells. Our data suggest that endogenous BH3-only protein induction may not be able to compensate for the high expression of antiapoptotic Bcl-2 family proteins in anoxia-resistant astrocytomas. They also support the conjecture that BH3 mimetics may represent an exciting new approach for the treatment of malignant glioma.

Neoplasia (2008) 10, 873–885

Introduction

Gliomas are the most common and malignant primary brain tumors in humans and are among the most hypoxic tumors known [1–3]. Uncontrolled growth, irregularities in the architecture of blood vessels, and tumor vessel occlusion through thrombosis are the main causes of tumor hypoxia [4–8]. In human glioma, the severity of tumor hypoxia is known to strongly correlate with malignancy and World Health Organization grade [1,2]. Glioblastoma multiforme, the highest-grade glioma, is characterized by large necrotic areas within the tumor tissue, and the appearance of necrosis correlates with enhanced therapy resistance, increased invasiveness, and a worse prognosis for the patients [1,2,6]. Because hypoxia provides a selection pressure for cells more tolerant to low oxygen concentrations, adaptive mechanisms to escape hypoxia-induced cell death likely play a pivotal role in gliomagenesis and tumor resistance.

Activation of the transcription factor hypoxia-inducible factor is known to play a central role in the transcriptional stress response to hypoxia [8,9]. This stress response enables cells to adapt their energy metabolism, to activate survival signaling pathways, to enhance vascular blood flow, and to increase oxygen transport [8]. However, prolonged, stringent hypoxia (anoxia) leads to mitochondrial dysfunction and

Abbreviations: PI, propidium iodide; LC3, light chain 3; MOMP, mitochondrial outer membrane permeabilization; TMRM, tetramethyl rhodamine methyl ester; STS, staurosporine

Address all correspondence to: Donat Kögel, PhD, Experimental Neurosurgery, Johann Wolfgang Goethe University Clinics, Theodor-Stern-Kai 7, Neuroscience Center, D-60590 Frankfurt am Main, Germany. E-mail: koegel@em.uni-frankfurt.de

[1]This study was supported by grants from the Wilhelm Sander Stiftung (grant 2005.067.1) to D.K. and from the Deutsche Forschungsgemeinschaft (PR 338/9-3 and 9/4) to J.H.M.P. and D.K.

[2]These authors contributed equally to this work.

Received 14 December 2007; Revised 21 May 2008; Accepted 21 May 2008

DOI 10.1593/neo.07842

the demise of cells, either by apoptosis or by nonapoptotic forms of cell death [10–13]. Pro- and antiapoptotic members of the Bcl-2 family are key regulators of hypoxia-induced cell death [13]. The Bcl-2 family proteins can be classified into three important subfamilies: 1) the BH3-only proteins that have only one domain in common, that is, the alpha helical BH3 domain; 2) the Bax-like proteins that contain three such domains (BH1, BH2, and BH3); and 3) the Bcl-2–like proteins that consist of four domains (BH1–4) [14,15]. Bax-like proteins (Bax, Bak, and potentially Bok) trigger mitochondrial permeabilization, which is required for the release of proapoptotic factors from mitochondria and for the activation of caspase-dependent and -independent cell death pathways [14,15]. In healthy cells, Bcl-2–like proteins inhibit the activation of Bax and Bak. However, BH3-only proteins can be induced in response to cellular or environmental stress, which neutralize Bcl-2–like proteins, activate Bax and Bak, and trigger cell death [16]. Among the diverse family of BH3-only proteins, in particular, BNIP3, NIX, PUMA, and Noxa have been implicated in hypoxia/anoxia–induced cell death [16–19].

It was previously proposed that glioma cell lines can be classified into "hypoxia-resistant" and "hypoxia-sensitive" cell lines [3,20]. Preservation of the clonogenic potential of glioblastoma cells after hypoxia depended on maintenance of a stable mitochondrial membrane potential and stable ATP levels [20]. However, the contribution of deregulated apoptotic signaling pathways for enhanced hypoxia resistance of malignant gliomas has not been investigated in detail. Here, we characterized the sensitivity of a panel of human glioma cell lines to anoxic stress and demonstrate that glioma cell lines exhibit a wide range of anoxia tolerance with high resistance to anoxia stringently correlating with enhanced expression levels of Bcl-2–like proteins but not with the lack of induction of BH3-only proteins. Our data also reveal that anoxia resistance can be efficiently overcome by silencing expression of Bcl-2 and Bcl-xL and by application of small-molecule Bcl-2 and Bcl-xL antagonists/BH3 mimetics.

Materials and Methods

Materials

The caspase substrate acetyl-DEVD-7-amino-4-methylcoumarin was purchased from Bachem (Heidelberg, Germany). Tetramethyl rhodamine methyl ester (TMRM) was purchased from MobiTec (Goettingen, Germany). C2-ceramide and BH3 mimetics BH3I-2′ and HA14-1 were from Merck Biosciences (Darmstadt, Germany) Lysotracker Red was from Invitrogen (Karlsruhe, Germany). All other chemicals came in analytical grade purity from Sigma-Aldrich (Deisenhofen, Germany).

Cell Lines and Culture

For this study, a panel of 17 human grade III to grade IV malignant astrocytoma cell lines was used. Glioma cell lines A172, U87, U251, U343, and U373, as well as the newly established glioma cell lines MZ-18, MZ-51, MZ-294, MZ-257, MZ-226, MZ-54, MZ-159, MZ-304, MZ-373, MZ-256, MZ-327, and MZ-348 [21], were grown in DMEM with 10% heat-inactivated fetal calf serum, 100 U/ml penicillin, and 100 mg/ml streptomycin and were maintained in a humidified incubator at 37°C and 5% CO_2. HeLa cells were grown and maintained under the same conditions as described for human glioma cell lines.

Anoxia Treatment

Cells were plated in 24-well plates at an optical density of approximately 40%. After 24 hours, cells were placed into an anoxic chamber (GasPak 100; Becton-Dickinson, Heidelberg, Germany) that was sealed and kept at 37°C. Severe hypoxic conditions (<0.1% O_2), here referred to as anoxia, were reached after approximately 60 minutes as indicated by a methylene blue indicator (Becton-Dickinson) placed inside the chamber.

Construction and Transfection of Expression Plasmids

Total human cDNA was obtained from U87 glioma cells. Primers 5′-ATA TAT AGA TCT ATG TCG CAG AAC GGA GCG CCC 3′ and 5′-ATA TAT GAA TTC TCA AAA GGT GCT GGT GGA GGT-3′ were used to generate full-length cDNA encoding *BNIP3* by polymerase chain reaction (PCR). In addition, a 5′- and 3′-end truncated deletion mutant of *BNIP3* (aa 49–164) lacking the N-terminus and the C-terminal transmembrane region was generated as a negative control with primers 5′-ATA TAT AGA TCT GCA CAG CAT GAG TCT GGA CGG-3′ and 5′-ATA TAT GAA TTC TCA AAC TTT CAG AAA TTC TGC AGA-3′. After restriction digestion with *Eco*RI and *Bgl*II, the inserts were ligated in-frame into *Eco*RI/*Bgl*II–digested pGFP-C1 expression vectors (Clontech, BD Biosciences, Heidelberg, Germany). Expression plasmid green fluorescent protein (GFP)–light chain 3 (LC3) was described elsewhere [22]. All expression constructs used in this study were transfected into cells using Metafectene reagent according to the manufacturer's instructions (Biontex, Martinsried/Planegg, Germany).

Fluorescence Microscopy

To allow efficient expression of GFP fusion proteins, cells were incubated for 24 hours after transfection before any further treatments. For microscopical analysis, cells were fixed and stained with the chromatin-specific dye Hoechst 33258 at a concentration of 1 μg/ml. For immunostaining of cytochrome *C*, a monoclonal anti–cytochrome *C* antibody (clone 6h2.b4; BD Biosciences) and a Texas Red–conjugated secondary antibody were used. Evaluation of the subcellular distribution of GFP fusion proteins (GFP-LC3 and GFP-Bnip3) and mitochondrial release of cytochrome *C* was performed by epifluorescence microscopy using an Eclipse TE 300 inverted microscope and a 40× objective (Nikon, Düsseldorf, Germany) equipped with the appropriate filter set (for GFP fluorescence: excitation of 465–495 nm, dichroic mirror of 505 nm, and emission of 515–555 nm; for Hoechst fluorescence: excitation of 340–380 nm, dichroic mirror of 400 nm, and emission of 435–485 nm; for Texas Red fluorescence: excitation of 540–580 nm, dichroic mirror of 595 nm, and emission of 600–660 nm). For analysis of the subcellular distribution of GFP-BNIP3, a total number of 300 cells were analyzed in three subfields for each culture. All experiments were performed at least three times with similar results.

Real-Time Quantitative PCR

Extraction of total cellular RNA and reverse transcription was performed as previously described [23]. Each PCR (performed in triplicate) contained 10 μl of *Taq*Man Universal PCR Master Mix, 1 μl of 20× *Taq*Man Gene Expression Assay Mix (containing both primers and probes), and 7 μl of cDNA (30 ng) diluted in RNase-free water. A typical standard protocol for quantitative PCR (qPCR) consisted of incubating at 50°C for 2 minutes and 95°C for 10 minutes followed by 40 cycles at 95°C for 15 seconds and 60°C for 40 seconds. Data analysis was performed with the GeneAmp 5700 Sequence

Detection System (Applied Biosystems, Darmstadt, Germany). Expression differences in anoxia-treated cultures compared to the normoxic controls were considered significant when $P < .05$. Primer sequences are available on request from the authors.

Gene Silencing Using Small Interfering RNA

The following annealed double-stranded small interfering RNA (siRNA) from Dharmacon (Chicago, IL) were used: *Bcl-2* siGenome duplexes D-003307-01-0010 and D-003307-04-0010; *Bcl-xL* siGenome duplexes D-003458-01-0010 and D-003458-04-0010. Scrambled siCONTROL Nontargeting siRNA #1 D-001210-01-20 from Dharmacon was used as negative, nonsilencing control. Cells were transfected with 250 nM siRNA using Oligofectamine from Invitrogen as described by the manufacturer.

Sodium Dodecyl Sulfate–Polyacrylamide Gel Electrophoresis and Western Blot Analysis

Sodium dodecyl sulfate–polyacrylamide gel electrophoresis and Western blot analysis were performed as described elsewhere [23]. The resulting blots were probed with a mouse monoclonal anti-Bnip3 antibody diluted at 1:1000 (Abcam, Cambridge, UK), a rabbit polyclonal anti–Bnip3L/Nix antibody diluted at 1:500 (Calbiochem, Merck Biosciences), a mouse monoclonal anti–Bcl-2 antibody diluted at 1:50 (Santa Cruz Biotechnology, Heidelberg, Germany), a rabbit polyclonal anti–Bcl-xL antibody diluted at 1:500 (BD Biosciences), a rabbit polyclonal anti–Mcl-1 antibody diluted at 1:200 (Santa Cruz Biotechnology), a rabbit polyclonal anti-Bax antibody diluted at 1:200 (Upstate, NY), a rabbit polyclonal anti-Bak antibody diluted at 1:200 (Santa Cruz Biotechnology), or a mouse monoclonal anti–α-tubulin antibody diluted at 1:5.000 (clone DM 1A; Sigma).

Determination of Caspase-3–Like Protease Activity

Cells were lysed in 200 µl of lysis buffer [10 mM HEPES, pH 7.4, 42 mM KCl, 5 mM $MgCl_2$, 1 mM phenylmethylsulfonyl fluoride, 0.1 mM EDTA, 0.1 mM EGTA, 1 mM dithiothreitol, 1 µg/ml pepstatin A, 1 µg/ml leupeptin, 5 µg/ml aprotinin, 0.5% 3-(3-cholamidopropyldimethylammonio)-1-propane sulfonate]. Fifty microliters of this lysate was added to 150 µl of reaction buffer (25 mM HEPES, 1 mM EDTA, 0.1% 3-(3-cholamidopropyldimethylammonio)-1-propane sulfonate, 10% sucrose, 3 mM dithiothreitol, pH 7.5) and 10 µM of the fluorigenic substrate acetyl-DEVD-7-amido-4-methylcoumarin. Accumulation of AMC fluorescence was monitored for 1 hour using a high-throughput screening fluorescent plate reader (excitation of 380 nm and emission of 465 nm). Fluorescence of

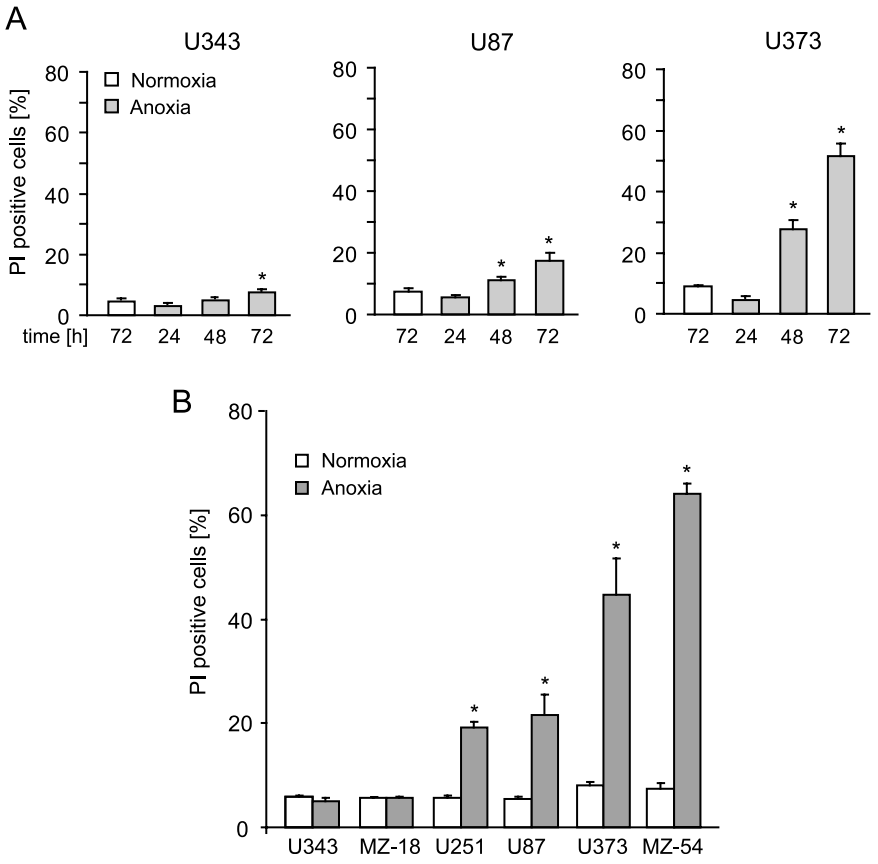

Figure 1. Malignant glioma cell lines display a high variability in anoxia sensitivity. (A) Cell lines U87, U343, and U373 were seeded at an optical density of approximately 40% confluence and were subjected to normoxia or anoxia for the indicated periods. Cell death was quantified by flow cytometric analysis of PI uptake. Data are means ± SEM from $n = 4$ cultures. *$P < .05$ compared to normoxic controls. Similar results were obtained in three separate experiments. (B) Cells of six cell lines with highly variable response to anoxia (see Table 1) were seeded at an optical density of approximately 40% confluence. After 24 hours, the cells were cultured under anoxic or normoxic conditions for 48 hours and were stained with Annexin V and PI. Cell death was determined using flow cytometry, summing up the percentage of Annexin V–, Annexin V/PI–, and PI-positive cells. Data are means ± SEM from $n = 4$ cultures. *$P < .05$ compared to normoxic controls. Similar results were obtained in three separate experiments.

Table 1. Glioma Cell Lines Show a Highly Variable Response to Anoxic Stress.

Cell Line	Fold Cell Death *vs* Control	SEM
MZ-18	**1**	**0.12**
U343	**1.2**	**0.14**
MZ-348	1.3	0.17
MZ-290	1.5	0.13
MZ-256	1.7	0.2
MZ-373	1.7	0.24
MZ-159	2	0.3
MZ-294	2	0.28
MZ-327	2.1	0.31
MZ-257	2.4	0.08
MZ-304	2.6	0.31
U87	**3**	**0.28**
U251	**3.4**	**0.41**
U373	**3.9**	**0.75**
MZ-54	**3.9**	**0.23**
MZ-51	4.6	0.69
MZ-226	4.8	0.68

Cells were seeded at an optical density of approximately 30% confluence. After 24 hours, the cells were exposed to anoxia or were cultured under normoxic conditions for 48 hours, stained with PI, and dead cells were counted using flow cytometry. The amount of cell death for each cell line is given as the ratio between the percentage of dead cells cultured under anoxic conditions (48 hours) and the percentage of dead cells cultured under normoxic conditions. Cell lines marked in bold letters were subsequently analyzed in more detail (Figure 1).
Data are means ± SEM from $n = 4$ independent cultures.

blanks containing no cell lysate was subtracted from the values. Protein content was determined using the Pierce Coomassie Plus Protein Assay reagent (KMF, Cologne, Germany). Caspase activity is expressed as change in fluorescence units per microgram protein per hour.

Flow Cytometry

For cell death analysis, cells were stained with Annexin V–FLUOS/propidium iodide (PI; Roche Applied Science, Mannheim, Germany) after treatments according to the manufacturer's instructions and flow cytometric analysis. For the analysis of $\Delta\Psi_m$, cells were stained with 30 nM TMRM for at least 15 minutes followed by flow cytometric analysis. To quantitatively detect changes in the extent of autophagy, acidic vacuoles were stained with 25 nM Lysotracker Red for 30 minutes followed by flow cytometric analysis. In all cases, a minimum of 10^4 events per sample was acquired. Flow cytometric analysis were performed on a FACScan (BD Biosciences) followed by analysis using Cell Quest and WinMDI software.

Statistics

Data are given as means ± SEM. For statistical comparison, *t* test or one-way analysis of variance followed by Tukey's test were used

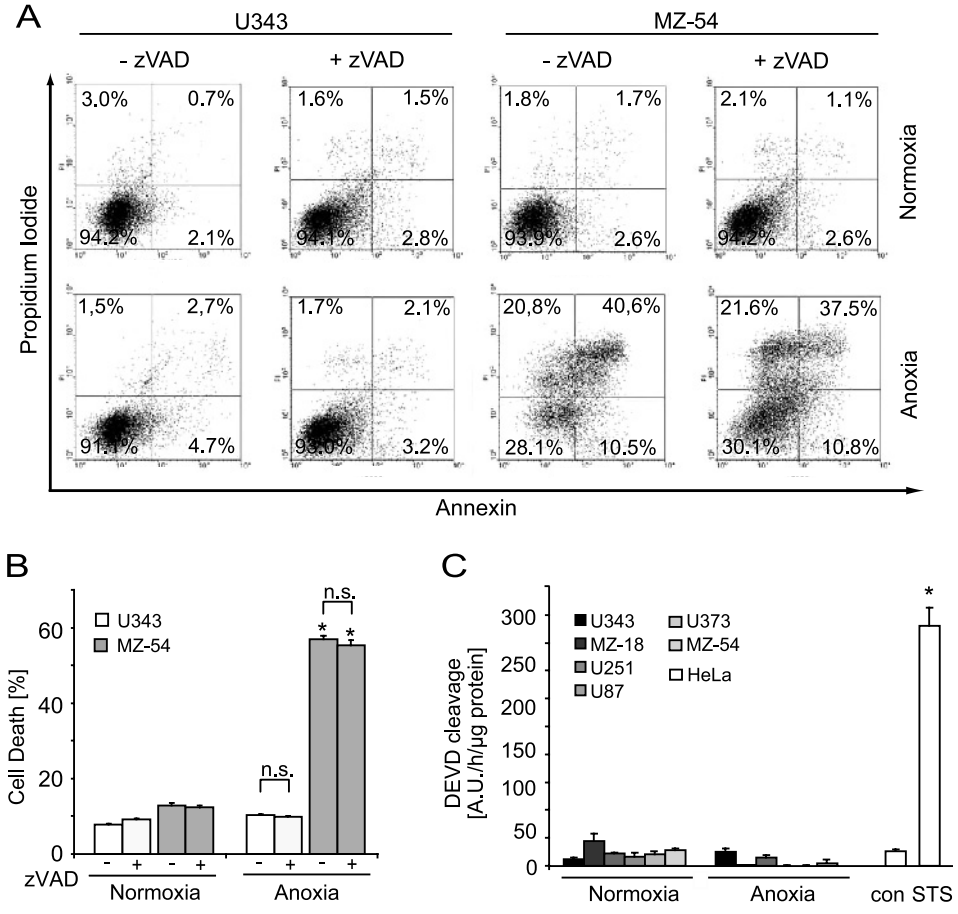

Figure 2. Anoxia induces a caspase-independent type of cell death in malignant glioma. (A) Representative dot plots and (B) cell death quantification of anoxia-resistant U343 and anoxia-sensitive MZ-54 cells. Cells were pretreated with zVAD (200 μM) for 2 hours. After 48 hours of normoxia or anoxia incubation in the presence or absence of zVAD, apoptosis was quantified with Annexin V/PI staining and flow cytometry. Data are means ± SEM from $n = 4$ independent cultures. *$P < .05$ compared to DMSO-treated cells. (C) After exposure to normoxia or anoxia (48 hours), glioma cell lines U343, MZ-18, U251, U87, U373, and MZ-54 were subjected to caspase-3–like activity assays. As a positive control, HeLa cells were treated with vehicle (DMSO) or STS (3 μM, 6 hours). Data are means ± SEM from $n = 4$ independent cultures. *$P < .05$ compared to normoxic controls. *n.s.* indicates not significant. Similar results were obtained in three separate experiments.

using SPSS software (SPSS GmbH Software, Munich, Germany). *P* values < .05 were considered to be statistically significant.

Results

Malignant Glioma Cells Exhibit a High Diversity in Anoxia-Induced, Caspase-Independent Cell Death

To establish a paradigm to analyze the inherent resistance of malignant glioma to cell death induced by anoxia, we performed a series of time course experiments in glioma cell lines U87, U343, and U373 placed in an anoxic chamber (<0.1% O_2) for 24, 48, and 72 hours, followed by flow cytometry analysis of PI uptake (Figure 1*A*). Propidium iodide uptake indicates loss of plasma membrane integrity that occurs during necrosis and, in the absence of phagocytosis, also as a secondary event after apoptosis. Forty-eight hours of anoxia lead to significant cell death in two of the investigated cell lines and was defined as the optimal time point for cell death quantification. Subsequent exposure of a panel of 17 glioma cell lines to anoxic stress for 48 hours revealed drastic differences in the sensitivity of the individual cell lines to anoxia-induced cell death (summarized in Table 1). Six cell lines with a wide range of anoxia sensitivity were selected for further investigation (Figure 1*B*). Cell lines U343 and MZ-18 were completely resistant to 48 hours of anoxia, whereas cell lines U373 and MZ-54 were particularly vulnerable (Figure 1*B*). Glucose deprivation (cultivation in glucose-free culture medium) and acidosis (pH 5.0, in HEPES-buffered culture medium supplemented with lactate) enhanced anoxia-dependent cell death but had no discernible effect on the pattern of sensitivity between the different cell lines (data not shown).

Application of the general caspase inhibitor zVAD did not diminish anoxia-induced cell death in anoxia-sensitive MZ-54 cells (Figure 2, *A* and *B*), which also was not associated with significant Annexin V binding in those cells that retained their membrane integrity (~10%). Anoxia also did not induce detectable effector caspase activity in anoxia-sensitive (or anoxia-resistant) cell lines, indicating that anoxia-triggered cell death occurred in a caspase-independent manner (Figure 2*C*). Collectively, these data suggested that anoxia did not induce classic apoptosis (type I cell death) in anoxia-sensitive glioma cells [12]. In contrast, exposure to the apoptosis-inducing kinase inhibitor staurosporine (STS) induced caspase activation in HeLa cells that were used as a control. Interestingly, anoxia-induced cell death was associated with cell shrinkage, chromatin condensation, and vesicular localization of the autophagosomal marker GFP-LC3 in MZ-54 cells (Figure 3*A*, *arrows*), suggesting that these cells activated autophagic pathways that have been shown to contribute to cell death in several paradigms (type II cell death) [24–26]. Quantitative analysis revealed that ~50% of MZ-54 cells displayed vesicular localization of GFP-LC3 after 48 hours of anoxia, whereas the percentage of U343 cells undergoing autophagy remained stable (Figure 3*B*). Inhibition of caspases with zVAD had no effect on the number of MZ-54 cells undergoing autophagy (Figure 3*B*).

Bax Translocation and Mitochondrial Depolarization in Anoxia-Sensitive Glioma Cells

Cells lacking expression of Bax and Bak display a potent resistance against anoxia-induced cell death, suggesting the involvement of the mitochondrial apoptosis pathway [11]. Activation of this pathway involves mitochondrial membrane permeabilization and the release of cytochrome *C*, an event that is accompanied by mitochondrial depolarization [14]. To analyze the correlation between anoxia sensitivity and mitochondrial dysfunction, we next investigated the effect of anoxia on the mitochondrial membrane potential ($\Delta\Psi_m$) by flow cytometry analysis of TMRM uptake (Figure 4*A*). HeLa cells that were used as a positive control showed a complete loss of $\Delta\Psi_m$ after 48 hours of anoxia as well as after treatment with the protein kinase inhibitor STS that served as an additional control. In all the investigated glioma cell lines, the ability to retain $\Delta\Psi_m$ after 48 hours of anoxia directly correlated with their resistance to cell death (Figures 4*A* and 1*B*), such that highly resistant U343 showed

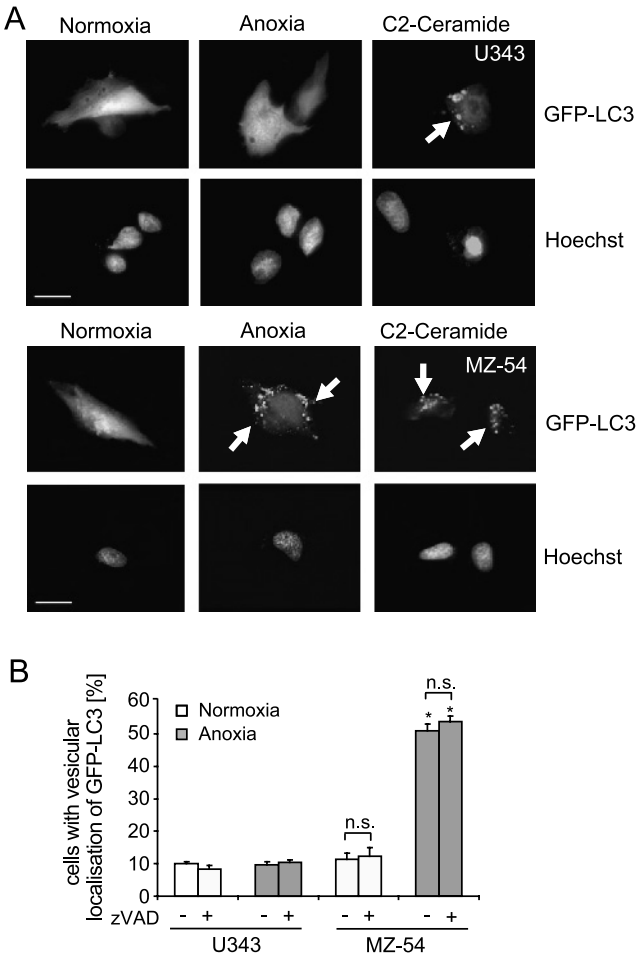

Figure 3. Anoxia-induced cell death is associated with autophagy in anoxia-sensitive glioma cells. (A) U343 cells (upper panel) and MZ-54 cells (lower panel) were transfected with a plasmid encoding GFP-LC3. Twenty-four hours after transfection, the cells were subjected to anoxia for 48 hours. As a positive control for the induction of autophagy, cells were also treated with 25 μM C2-Ceramide for 24 hours. After fixation, cells were stained with Hoechst 33258 and analyzed by epifluorescence microscopy. Experiments were repeated two times with similar results. Scale bar, = 10 μm. (B) Quantitative evaluation of glioma cells containing GFP-LC3–positive autophagosomes. Anoxia-resistant (U343) and anoxia-sensitive (MZ-54) cell lines were transfected with a plasmid encoding GFP-LC3. Twenty-four hours after transfection, cells were pretreated with the caspase-inhibitor zVAD (200 μM) and were cultured for an additional 48 hours under normoxic and anoxic conditions. Similar results were obtained in two separate experiments. Data are means ± SEM from $n = 4$ independent cultures. *$P < .05$ compared to normoxic controls. *n.s.* indicates not significant compared to respective treatment in the absence of zVAD.

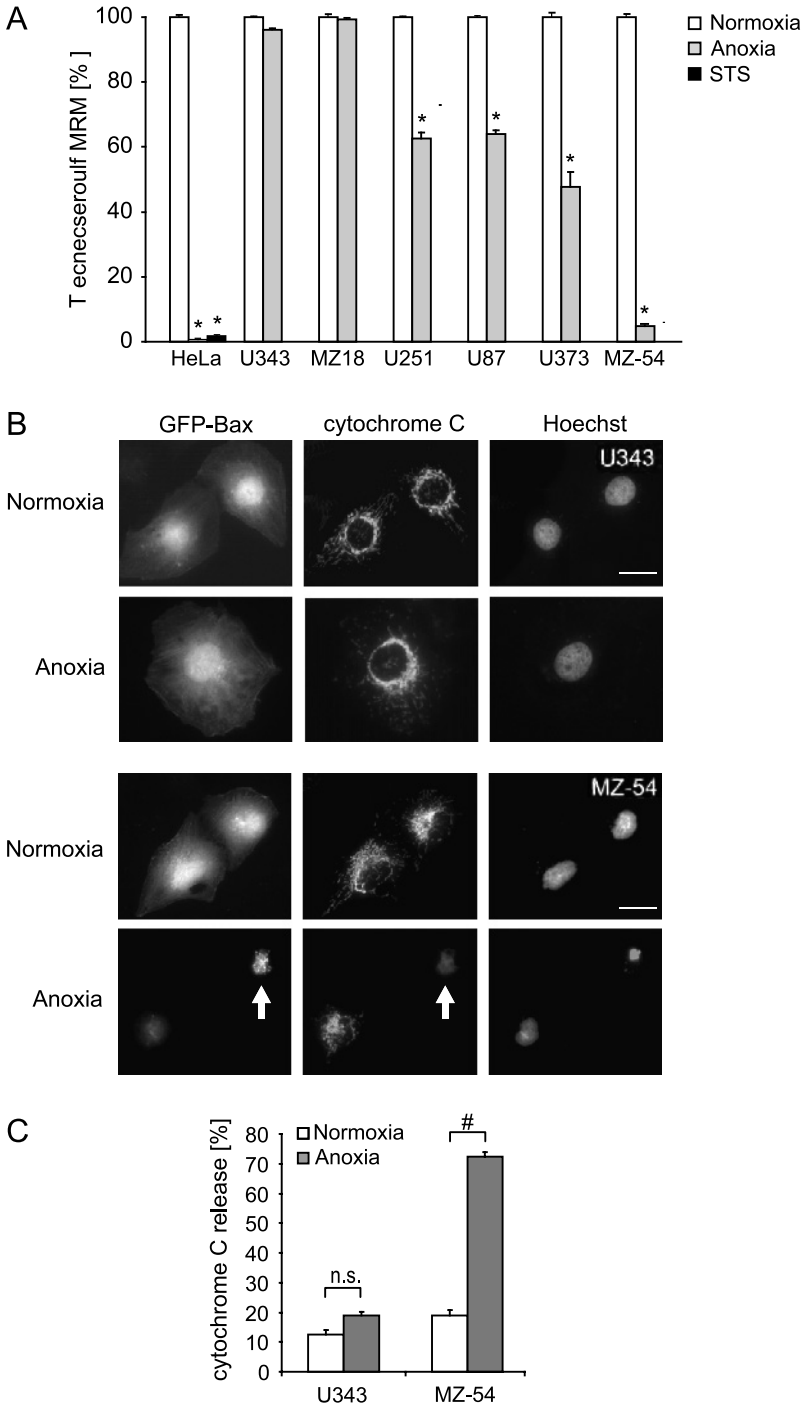

Figure 4. Anoxia induces mitochondrial dysfunction and Bax translocation in anoxia-sensitive glioma cells. (A) Glioma cell lines U343, MZ-18, U251, U87, U373, and MZ-54 were exposed to normoxia, anoxia (48 hours), or were treated with 5 μM STS (24 hours) and subsequently stained with TMRM after which TMRM fluorescence was measured by flow cytometry. HeLa cells served as controls. Data are given as the percentage of fluorescence retained in comparison to the control of each respective cell line (normoxia). Data are means ± SEM from $n = 4$ independent cultures. $^{*}P < .05$ compared to normoxic control. Similar results were obtained in two separate experiments. (B) Translocation of GFP-tagged Bax in anoxia-sensitive glioma cells under anoxic conditions. Twenty-four hours posttransfection with GFP-Bax, U343 (upper panel) or MZ-54 cells (lower panel) were exposed to anoxia or were cultured under normoxic conditions for 24 hours. After fixation, immunostaining of cytochrome *C* and staining of nuclei with Hoechst 3342 (1 μg/μl), cells were analyzed by fluorescence microscopy. Scale bar, 10 μm. (C) Quantification of cells displaying cytochrome *C* release in U343 and MZ-54 cultures during anoxia-induced cell death. Data are means ± SEM from $n = 4$ independent cultures. $^{\#}P < .05$ compared to normoxic controls. *n.s.* indicates not significant.

no mitochondrial depolarization and highly vulnerable MZ-54 cells nearly complete mitochondrial depolarization.

Mitochondrial permeabilization and depolarization, as well as release of cytochrome *C*, are triggered by the posttranslational activation of Bax and Bak, involving translocation to mitochondria (Bax), membrane insertion, and oligomerization (both Bax and Bak). Transient overexpression of GFP-tagged Bax [27] demonstrated translocation and clustering of Bax during anoxia-induced cell death in the sensitive MZ-54 cells, whereas U343 showed no evidence of Bax activation (Figure 4*B*). In addition, MZ-54 cells with clustered Bax localization displayed drastic cell shrinkage, chromatin condensation, and cytochrome *C* release during anoxia-induced cell death (Figure 4*B*, *arrow*). Quantitative analyses indicated that most of the MZ-54 cells had released their cytochrome *C* after 48 hours of anoxia (Figure 4*C*).

Expression and Hypoxia-Dependent Induction of BNIP3 and Nix Does Not Correlate with Anoxia Sensitivity of Glioma

Because the BH3-only genes *BNIP3* and *NIX* have been reported to play important roles in hypoxia-dependent cell death [19] and because both genes might act as tumor suppressors [28], we asked whether loss of expression and/or induction of these genes may contribute to the observed resistance to cell death, mitochondrial depolarization, and Bax translocation. Lack of expression and/or anoxia-dependent induction of BNIP3 and NIX occurred only in a small subset of the cell lines investigated (Figure 5*A*). Importantly, there was no clear correlation between BNIP3 and NIX protein expression and the previously observed sensitivity to anoxia in the six cell lines that we had chosen to investigate in more detail (Figure 1*B*) or in the other glioma cell lines investigated (Table 1). Indeed, robust induction of BNIP3 and/or NIX was detected in both anoxia-sensitive (e.g., MZ-54 and U373) and -resistant (e.g., MZ-18) cells. To analyze the potential contribution of *BNIP3* and *NIX*, as well as of *PUMA* and *Noxa*, two other BH3-only genes known to be transcriptionally induced under hypoxic/anoxic conditions [16–19], we performed additional real-time qPCR analysis. All four genes were induced by anoxia both in MZ-54 and in U343 cells (Figure 5*B*). *BNIP3* and *NIX* were potently induced in anoxia-resistant U343 cells and in anoxia-sensitive MZ-54 cells. *Noxa* was induced ~50-fold in anoxia-resistant, wild type p53–expressing U343 cells [29]. The observed marginal induction of *Noxa* in anoxia-sensitive MZ-54 cells may suggest that these cells do not express functional p53 but retain the ability to potently induce

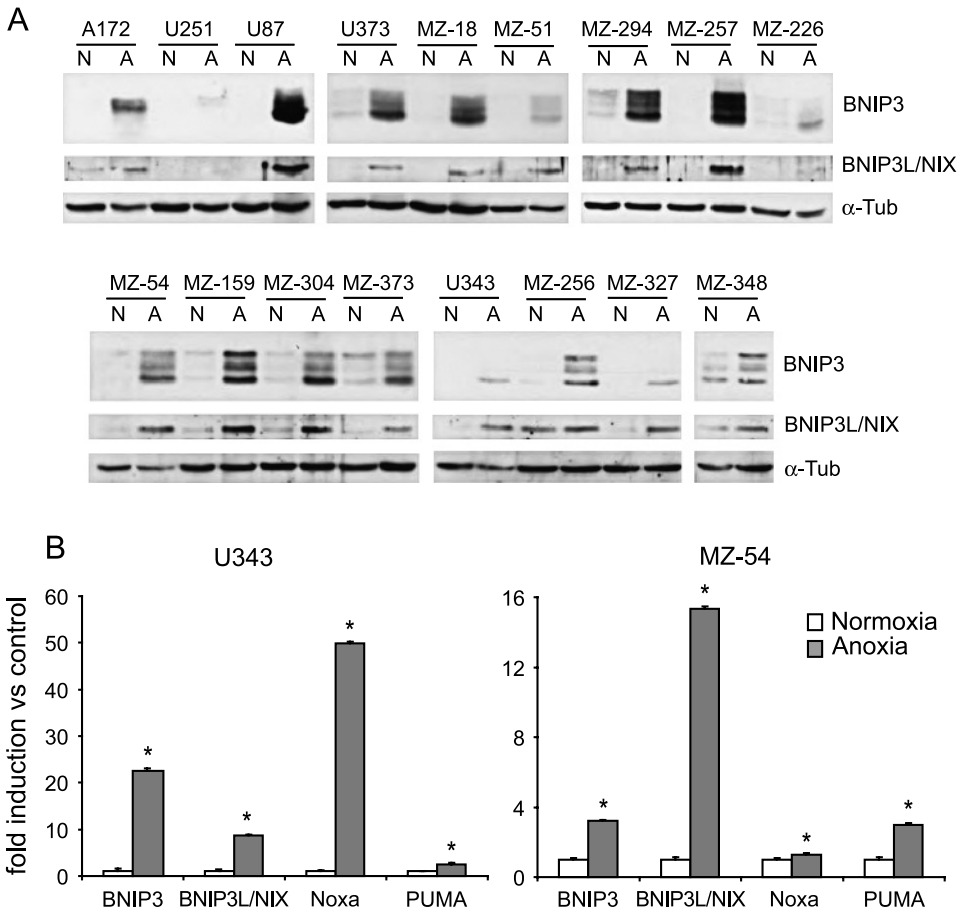

Figure 5. Induction of BH3-only genes in anoxia-sensitive and anoxia-resistant glioma cells. (A) Western blot analysis of BNIP3 and BNIP3L/NIX induction after 48 hours of anoxia. The indicated glioma cell lines were cultured under normoxic (N) and anoxic (A) conditions for 48 hours, and whole-cell lysates were probed with antibodies against BNIP3 and BNIP3L/NIX. α-Tubulin served as a loading control. (B) Expression analysis of BH3-only genes by qPCR. U343 and MZ-54 cells were cultured for 24 hours under anoxic or normoxic conditions, after which total RNA was analyzed by real-time qPCR. Expression analysis of BH3-only transcripts BNIP3, BNIP3L/NIX, Noxa, and Puma was performed by 40 cycles each. TATA-binding protein served as an internal control (40 cycles). Data are means ± SEM from $n = 4$ independent cultures. *$P < .05$ compared to normoxic controls. Similar results were obtained in three separate experiments.

BNIP3, *NIX*, and *PUMA* in a p53-independent manner. Collectively, the data obtained from the Western blot and real-time qPCR experiments suggest that anoxia resistance of many glioma cell lines did not result from a lack of activation of known BH3-only proteins that act as upstream activators of the mitochondrial pathway of apoptosis.

High Levels of Antiapoptotic Bcl-2 Family Protein Expression in Anoxia-Resistant Malignant Glioma: Failure to Reactivate Cell Death by Ectopic Expression of BNIP3

Because malignant gliomas have been shown to overexpress antiapoptotic Bcl-2 family members [30], we next investigated the relative expression levels of Bcl-2, Bcl-xL, and Mcl-1 in glioma cells. Interestingly, among the six cell lines investigated in more detail, the anoxia-sensitive cells revealed low expression levels of Bcl-xL (MZ-54, U373), Bcl-2 (MZ-54, U373, U87, U251), or Mcl-1 (U373; Figure 6, *upper panel*). Conversely, the expression of Bcl-2, Bcl-xL, and Mcl-1 was robust and at high levels in U343 and MZ-18, the two cell lines showing the highest resistance to anoxia. In contrast to antiapoptotic Bcl-2 family members, there was no clear correlation between expression levels of proapoptotic Bcl-2 family members, as lysates of both MZ-54 cells and U343 cells displayed very similar protein levels of Bax and Bak (Figure 6, *lower panel*).

We next addressed the question whether overexpression of the hypoxia-inducible BH3-only protein BNIP3 was able to reactivate cell death in the anoxia-resistant U343 cells. To this end, we ectopically overexpressed GFP-tagged BNIP3 in U343 cells and in the anoxia-sensitive MZ-54 cells. Expression of BNIP3 under normoxic conditions had no major effects on cell death in both cell lines (Figure 7*A*). Because additional hypoxia-induced mechanisms might be required to activate overexpressed BNIP3 on the posttranslational level, we also analyzed the effect of Bnip3 overexpression on cell death under anoxic conditions that lead to a significant increase over normoxic control transfections in anoxia-sensitive MZ-54 cells but not in anoxia-resistant U343 cells (Figure 7*A*). Further analysis revealed that GFP-BNIP3 was mostly retained in the nucleus of U343 cells [31] (Figure 7, *B* and *C*) but was translocated to the mitochondria in a large fraction of MZ-54 cells subjected to anoxia, suggesting that BNIP3-triggered cell death is controlled by additional steps during anoxia. Because BNIP3 was previously implicated in the regulation of autophagic pathways, we also analyzed the effects of BNIP3 overexpression on the cellular content of acidic vacuoles (Figure 7*D*). Indeed, ectopically overexpressed BNIP3 lead to significantly increased Lysotracker Red signals under both normoxic and anoxic conditions in MZ-54 cells, whereas autophagy was only moderately increased in anoxic but not in normoxic U343 cells (Figure 7, *D* and *E*).

BH3 Mimetics Reactivate Anoxia-Triggered Cell Death and Autophagy in Otherwise Resistant Glioma

Because ectopic BNIP3 overexpression was not able to fully reactivate anoxia-induced cell death in U343 cells, we next asked the question whether pharmacological inhibition of antiapoptotic Bcl-2 family members would resensitize glioma cells to anoxia-triggered cell death. To inhibit Bcl-2 and Bcl-xL pharmacologically, we used two different cell-permeable small-molecule inhibitors. The BH3 mimetic BH3I-2′ was previously shown to bind to both Bcl-2 and Bcl-xL [32,33], whereas HA14-1 has been described as a specific inhibitor of Bcl-2 [34]. Both BH3 mimetics were used at a subtoxic concentration of 30 μM (data not shown) and were capable of significantly potentiating anoxia-triggered cell death in anoxia-sensitive

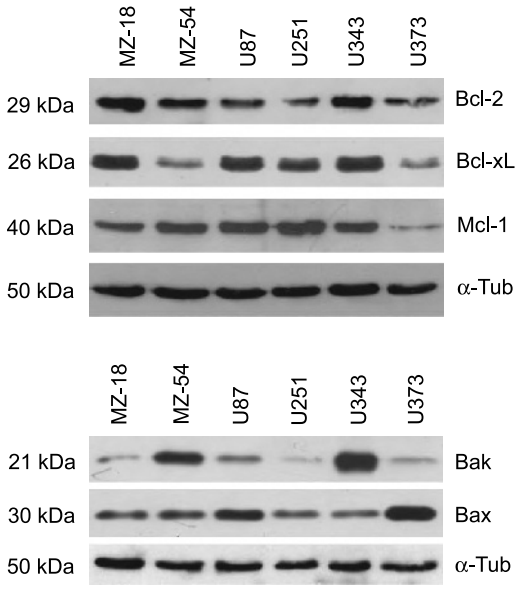

Figure 6. Analysis of expression levels of pro- and antiapoptotic Bcl-2 family members in six glioma cell lines by Western blot analysis. Whole-cell lysates were probed with antibodies against Bcl-2, Bcl-xL, and Mcl-1 (antiapoptotic members) and against Bak and Bax (proapoptotic members). α-Tubulin served as a loading control. Similar results were obtained in two separate experiments.

MZ-54 cells (Figure 8, *A* and *B*). Interestingly, both BH3 mimetics were also able to reactivate anoxia-triggered cell death in otherwise anoxia-resistant U343 cells (Figure 8, *A* and *B*). We also analyzed the effects of BH3 mimetics on the induction of autophagy under normoxic and anoxic conditions (Figure 9, *A* and *B*). Both HA14-1 and BH3I-2′ were capable of enhancing anoxia-triggered autophagy in MZ-54 cells and U343 cells (Figure 9*B*).

Specific Inhibition of Bcl-2 Family Members by RNA Interference

To dissect the specific roles of protective Bcl-2 family members in anoxia resistance of glioma, we performed a series of RNA interference experiments (Figure 10, *A* and *B*). Western blot analysis revealed that protein levels of both Bcl-2 and Bcl-xL potently could be downmodulated in anoxia-resistant U343 cells and anoxia-sensitive MZ-54 cells (Figure 10, *A* and *B*). Similar to the death-promoting effects of BH3 mimetics, knockdown of both Bcl-2 and Bcl-xL was able to further enhance the sensitivity of MZ-54 cells to anoxic cell death and to reactivate anoxia-induced cell death in U343 cells (Figure 10, *A* and *B*). In contrast to RNA interference against Bcl-2 and Bcl-xL, silencing of Mcl-1 did not enhance anoxia-induced cell death in U343 cells (data not shown). In addition to its effects on anoxia-induced death, the knockdown of Bcl-xL also exerted significant cytotoxic effects under normoxic conditions in both glioma cell lines investigated. Similar effects, albeit to a lesser degree, were observed after knockdown of Bcl-2, suggesting that glioma cells might be addicted to the overexpression of protective Bcl-2 family members.

Discussion

Malignant gliomas are among the most hypoxic tumors known, and the extent of tumor hypoxia correlates with increasing World Health

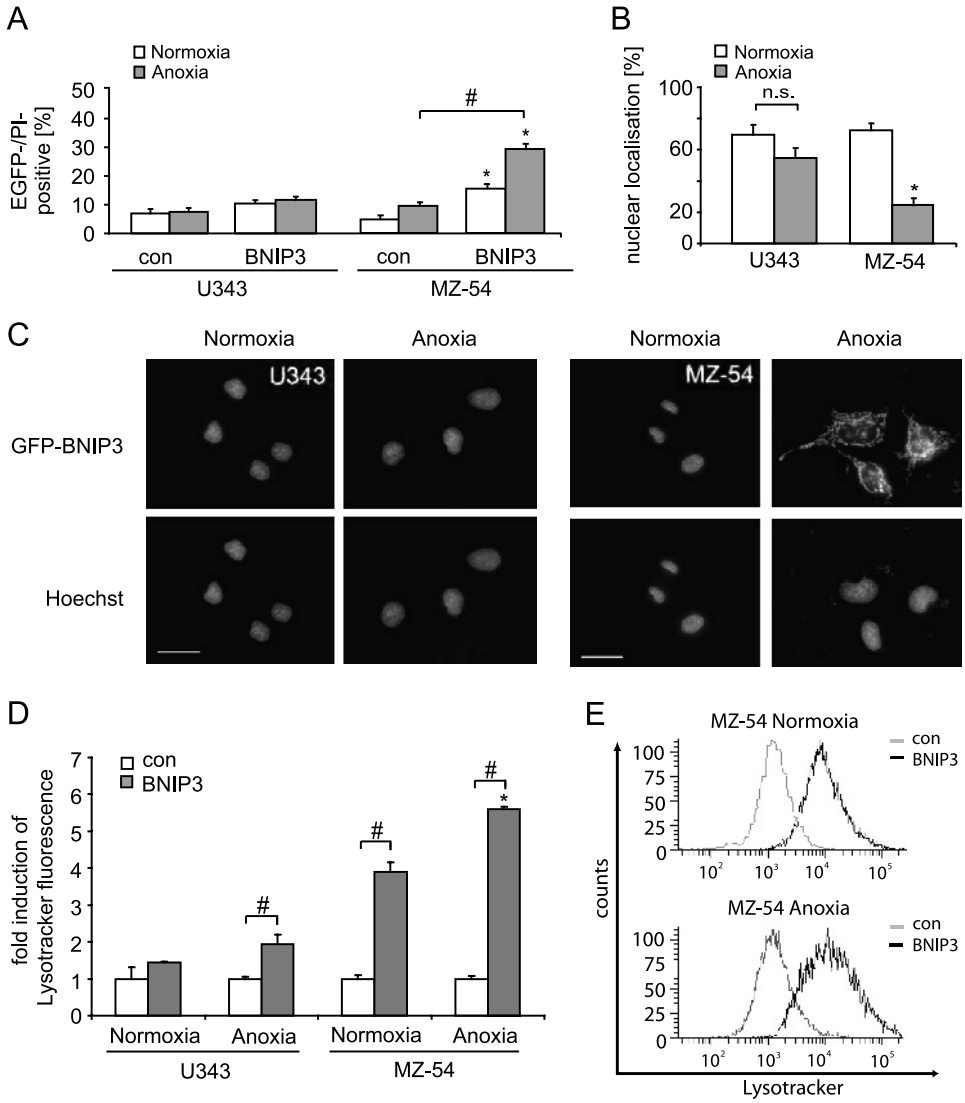

Figure 7. Ectopic overexpression of GFP-tagged BNIP3 induces cell death in anoxia-sensitive MZ-54 cells. (A) Twenty-four hours posttransfection with GFP-BNIP3, U343 and MZ-54 cells were exposed to anoxia or were cultured under normoxic conditions for another 24 hours, harvested, and stained with PI. Green fluorescent protein/PI–positive cells were identified with flow cytometric analysis. A truncated GFP-BNIP3 lacking the N-terminus and the C-terminal transmembrane domain served as negative control. Data are means ± SEM from $n = 4$ independent cultures. $^{*}P < .05$ compared to normoxic control. $^{\#}P < .05$, difference from respective normoxic control. (B) Quantitative analysis of cells with nuclear localization of GFP-BNIP3. Twenty-four hours posttransfection with GFP-BNIP3, U343 or MZ-54 cells were exposed to anoxia or were cultured under normoxic conditions for 24 hours, stained with Hoechst 3342 (1 μg/μl), and subjected to fluorescence microscopy. Data are means ± SEM from $n = 5$ independent cultures. $^{*}P < .05$ compared to the normoxic control. *n.s.* indicates not significant. (C) Mitochondrial translocation of BNIP3 during anoxia. U343 and MZ-54 cells were treated as described previously. Scale bar, 10 μm. (D) Lysosomal induction by transient overexpression of GFP-BNIP3 during anoxia. Twenty-four hours posttransfection with GFP-BNIP3 or tBNIP3 (control), U343 and MZ-54 cells were exposed to anoxia or were cultured under normoxic conditions for 24 hours. Cells were trypsinized, stained with Lysotracker Red DND-99, and GFP-positive cells were analyzed by flow cytometry. Data are given as fold change *versus* control-transfected, normoxic cultures of the respective cell line. Data are means ± SEM from $n = 4$ independent cultures. $^{*}P < .05$ compared to normoxic control. $^{\#}P < .05$, difference from cells transfected with the tBnip3 control plasmid. Representative FACS profiles obtained after Lysotracker Red staining of MZ-54 cells are shown in (E).

Organization grade and clinical outcome [35–37]. Oxygen withdrawal exerts a negative selection pressure in tumor cells, and cellular adaptation to prolonged hypoxic/anoxic conditions leads to enhanced resistance to anoxia-triggered cell death [38]. Importantly, these adaptive mechanisms possibly represent a major driving force for the development of cross-resistance of tumor cells against other death stimuli [37,39,40]. Despite the fact that glioma cells, in general, are highly tolerant to hypoxic conditions [41], our initial experiments in a set of 17 glioma cell lines demonstrate that malignant gliomas nonetheless exhibit a wide range of anoxia resistance.

Members of the Bcl-2 family are key regulators of the mitochondrial pathway of apoptosis that encompasses the release of cytochrome *C* from the mitochondria and plays a pivotal role in cell death triggered by anoxia [10,11,13]. However, in line with previous observations [12], anoxia induced a caspase-independent type of cell

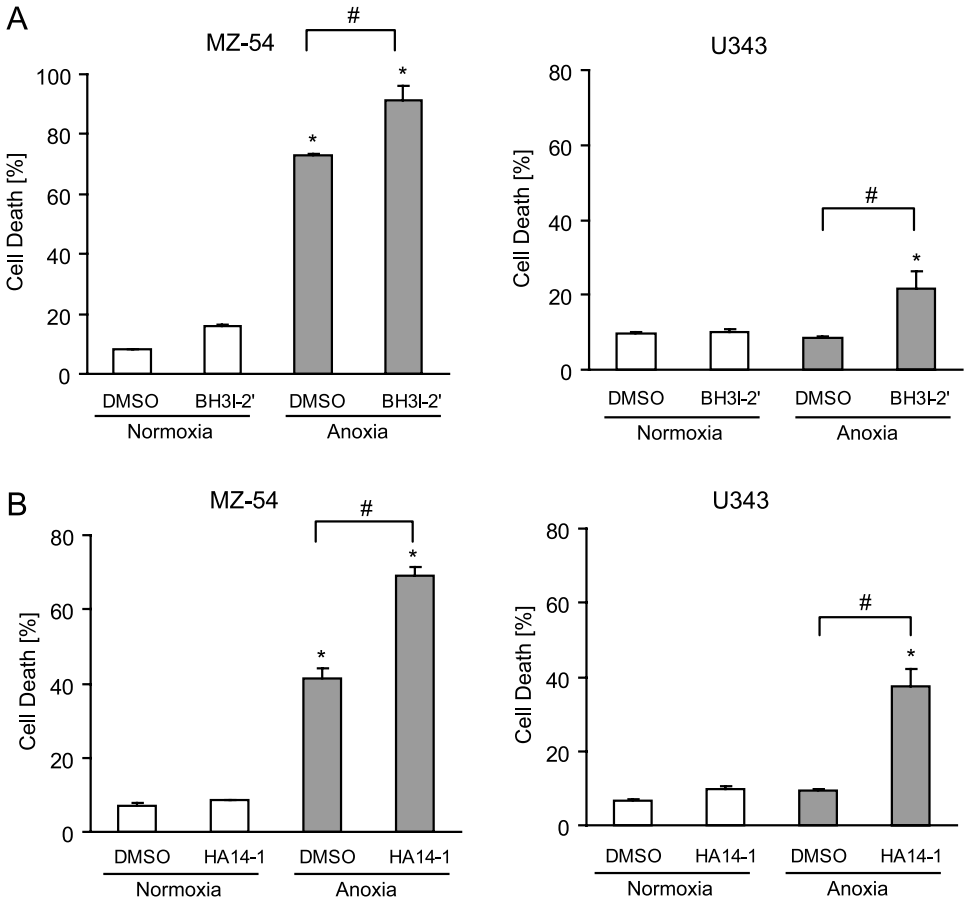

Figure 8. Inhibition of Bcl-2 and Bcl-xL reactivates anoxia-induced cell death in anoxia-resistant glioma cells. U343 and MZ-54 cells were pretreated with 20 μM BH3I-2′ (A) and 30 μM HA14-1 (B) for 1 hour. Afterward, the cells were subjected to anoxia for 48 hours or were cultured under normoxic conditions. Cells were stained with Annexin V and PI, and cell death was determined with flow cytometry. Data are means ± SEM from $n = 4$ independent cultures. *$P < .05$ compared to normoxic control. Similar results were obtained in at least two separate experiments.

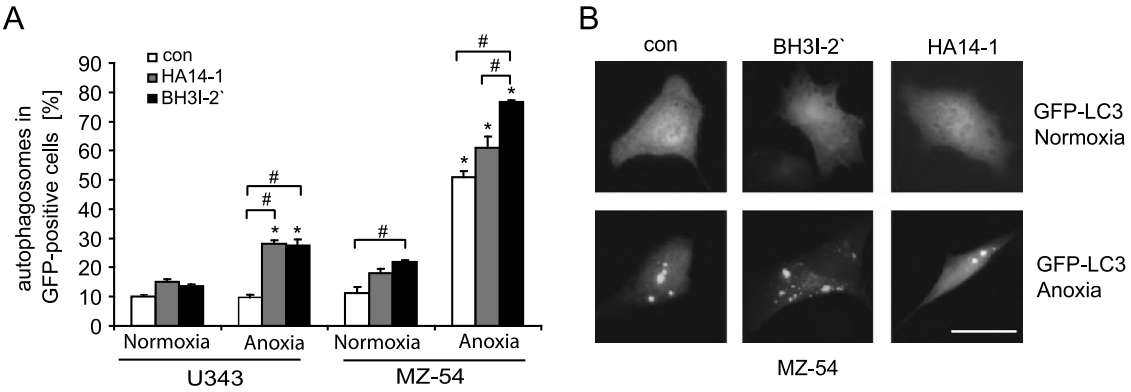

Figure 9. BH3 mimetics increase the number of cells containing GFP-LC3–positive autophagosomes under anoxia. (A) Anoxia-resistant (U343) and anoxia-sensitive (MZ-54) cell lines were transfected with a plasmid encoding GFP-LC3. Twenty-four hours after transfection, cells were pretreated with 20 μM BH3I-2′ and 30 μM HA14-1 for 1 hour and were cultured for an additional 48 hours under normoxic and anoxic conditions. Data are means ± SEM from $n = 4$ independent cultures. *$P < .05$ compared to normoxic control. #$P < .05$ compared to the respective treatment without the addition of BH3 mimetics. Similar results were obtained in at least two separate experiments. (B) Representative images of MZ-54 cells undergoing autophagy. Cells were treated as described previously, fixed, and subcellular localization of GFP-LC3 was analyzed by fluorescence microscopy. Scale bar, 10 μm.

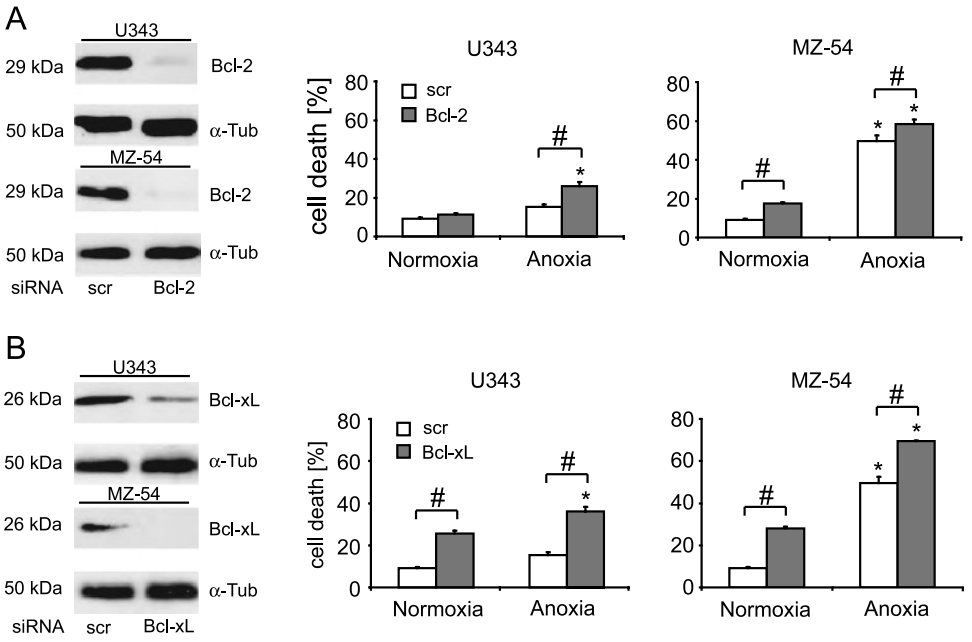

Figure 10. Specific knockdown of antiapoptotic Bcl-2 family members by RNA interference leads to increased cell death under anoxic conditions. Anoxia-resistant (U343) and anoxia-sensitive (MZ-54) cell lines were transfected with scrambled control siRNA, Bcl-2 siRNA, or Bcl-xL siRNA. Knockdown of Bcl-2 (A) and Bcl-xL (B) was confirmed by Western blot analysis, with α-tubulin serving as a loading control. Knockdown of Bcl-2 and Bcl-xL leads to increased cell death in anoxia-sensitive MZ-54 cells and anoxia-resistant U343 cells under anoxic conditions. Cell death was quantified after 48 hours of anoxia by flow cytometric analysis by Annexin V/PI staining. Data are means ± SEM from $n = 4$ independent cultures. $^{\#}P < .05$ compared to scrambled siRNA control.

death in glioma cells. Of note, MZ-54 cells are sensitive to caspase-dependent apoptotic cell death induced by other proapoptotic stimuli such as the death ligand TRAIL [21], indicating that these cells retain the ability to induce effector caspases.

Although stimulation of autophagy may constitute a primordial protective stress response, overactivation of autophagy may also lead to autophagic type II cell death in many experimental paradigms [24,25]. In line with these findings, anoxia-induced cell death in glioma cells displayed characteristics of type II cell death, because it was associated with nuclear condensation, cell shrinkage, and translocation of GFP-tagged LC3 to autophagosomal vacuoles in anoxia-sensitive MZ-54 glioma cells. Additional experiments with ectopically expressed GFP-tagged Bax revealed that Bax was activated and translocated to the mitochondria during anoxia-triggered cell death, indicating that, under anoxic conditions, the intrinsic pathway of apoptosis was triggered upstream of the mitochondria. There is increasing evidence that both Bcl-2 and Bcl-xL play important roles in inhibition of autophagy [42–47], whereas mitochondria undergoing mitochondrial outer membrane permeabilization (MOMP) can stimulate autophagy [48]. In addition to their role in the inhibition of MOMP, Bcl-2 and Bcl-xL antagonize the activation of autophagy by directly sequestering the autophagy regulator Beclin through binding to its BH3 domain [44,46,47]. In light of these observations, the observed anoxia resistance in U343 cells and MZ-18 cells may be causally related to the inhibition of autophagy by Bcl-2 and Bcl-xL, both of which were strongly overexpressed in these cell lines. In support of this notion, anoxia-dependent cell death could be potently reactivated by BH3 mimetics and RNA interference against Bcl-2 and Bcl-xL in otherwise resistant U343 cells. Our data clearly indicate that induction of MOMP is a central step in anoxia-triggered cell death in glioma cells and that high levels of Bcl-2 and Bcl-xL might control several caspase-dependent and -independent pathways in malignant glioma.

Our Western blot and qPCR analyses indicated that the BH3-only genes *PUMA*, *Noxa*, *BNIP3*, and *NIX* were transcriptionally activated in anoxia-resistant U343 cells, thus providing evidence for the functional integrity of anoxia-induced apoptotic signaling pathways upstream of the mitochondria in these cells. However, activation of BH3-only genes was not sufficient to induce cell death in the presence of overexpressed Bcl-2 and Bcl-xL. Although ectopically overexpressed Bnip3 was translocated to the mitochondria and enhanced autophagy in anoxia-sensitive MZ-54 cells, it was mostly retained in the nucleus of anoxia-resistant U343 cells [31], indicating that posttranslational mechanisms might further account for the potent resistance to anoxia-dependent cell death in these cells.

Because our Western blot analyses had indicated a clear correlation between expression levels of antiapoptotic Bcl-2 family members and anoxia resistance, we asked the question whether inhibition of Mcl-1, Bcl-2, and Bcl-xL would lead to the reactivation of anoxia-induced cell death in otherwise anoxia-resistant glioma cells. Inhibition of Mcl-1 that was expressed at very low levels in one of the anoxia-sensitive cell lines (U373) had no discernible effect on anoxia-triggered cell death in anoxia-sensitive MZ-54 cells and anoxia-resistant U343 cells, indicating that Mcl-1 might play a minor role in anoxia tolerance of malignant glioma (data not shown). In contrast, inhibition of Bcl-2 and Bcl-xL by RNA interference was indeed capable of efficiently reducing the anoxia tolerance of glioma cells. Although our data indicate that both family members serve to protect glioma cells against anoxic stress, the extent of anoxic cell death in both MZ-54 and U343 cells was slightly higher after silencing of Bcl-xL. Of note, silencing of Bcl-xL and, to a lesser degree, of Bcl-2 also enhanced cell death under normoxic conditions, suggesting that overexpression of

protective Bcl-2 family members might be required to maintain the mitochondrial integrity of glioma cells in the absence of metabolic stress, thus resulting in oncogenic addiction.

To pharmacologically inhibit Bcl-2 and Bcl-xL, we used the BH3 mimetic BH3I-2′, which was previously shown to bind to both Bcl-2 and Bcl-xL [32,33], and the BH3 mimetic HA14-1, which has been described as a specific inhibitor of Bcl-2 [34]. Interestingly, both small-molecule inhibitors significantly potentiated anoxia-triggered cell death in anoxia-sensitive MZ-54 cells. Importantly, both BH3 mimetics were also able to reactivate anoxia-triggered cell death in otherwise anoxia-resistant U343 cells, suggesting that pharmacological inhibition of both Bcl-2 and Bcl-xL might be an efficient strategy to potentiate caspase-independent cell death in glioma. In this context, it is worth mentioning that a potent resistance against classic caspase-dependent apoptosis is a major hallmark of malignant gliomas [49], and the antitumorigenic effects of currently used antiglioma therapies such as temozolomide and gamma irradiation are largely based on the induction of caspase-independent cell death [50,51].

In conclusion, our data emphasize the fundamental role of Bcl-2 and Bcl-xL in anoxia resistance of malignant glioma and highlight the enormous therapeutic potential of BH3 mimetics for the treatment of tumors highly resistant to caspase-dependent and -independent apoptosis.

Acknowledgments

The authors thank Hildegard Schweers for excellent technical assistance and Noboru Mizushima (The Tokyo Metropolitan Institute of Medical Science, Tokyo, Japan) and Tamotsu Yoshimori (National Institute of Genetics, Shizuoka, Japan) for providing the GFP-LC3 plasmid.

References

[1] Maher EA, Furnari FB, Bachoo RM, Rowitch DH, Louis DN, Cavenee WK, and DePinho RA (2001). Malignant glioma: genetics and biology of a grave matter. *Genes Dev* **15**, 1311–1333.

[2] Kleihues P, Louis DN, Scheithauer BW, Rorke LB, Reifenberger G, Burger PC, and Cavenee WK (2002). The WHO classification of tumors of the nervous system. *J Neuropathol Exp Neurol* **61**, 215–225; discussion 226–229.

[3] Turcotte ML, Parliament M, Franko A, and Allalunis-Turner J (2002). Variation in mitochondrial function in hypoxia-sensitive and hypoxia-tolerant human glioma cells. *Br J Cancer* **86**, 619–624.

[4] Carmeliet P and Jain RK (2000). Angiogenesis in cancer and other diseases. *Nature* **407**, 249–257.

[5] Yancopoulos GD, Davis S, Gale NW, Rudge JS, Wiegand SJ, and Holash J (2000). Vascular-specific growth factors and blood vessel formation. *Nature* **407**, 242–248.

[6] Rong Y, Durden DL, Van Meir EG, and Brat DJ (2006). "Pseudopalisading" necrosis in glioblastoma: a familiar morphologic feature that links vascular pathology, hypoxia, and angiogenesis. *J Neuropathol Exp Neurol* **65**, 529–539.

[7] Gatenby RA and Gillies RJ (2004). Why do cancers have high aerobic glycolysis? *Nat Rev Cancer* **4**, 891–899.

[8] Semenza GL (2003). Targeting HIF-1 for cancer therapy. *Nat Rev Cancer* **3**, 721–732.

[9] Bernaudin M, Nedelec AS, Divoux D, MacKenzie ET, Petit E, and Schumann-Bard P (2002). Normobaric hypoxia induces tolerance to focal permanent cerebral ischemia in association with an increased expression of hypoxia-inducible factor-1 and its target genes, erythropoietin and VEGF, in the adult mouse brain. *J Cereb Blood Flow Metab* **22**, 393–403.

[10] Papandreou I, Krishna C, Kaper F, Cai D, Giaccia AJ, and Denko NC (2005). Anoxia is necessary for tumor cell toxicity caused by a low-oxygen environment. *Cancer Res* **65**, 3171–3178.

[11] Shroff EH, Snyder C, and Chandel NS (2007). Bcl-2 family members regulate anoxia-induced cell death. *Antioxid Redox Signal* **9**, 1405–1410.

[12] Steinbach JP, Wolburg H, Klumpp A, Probst H, and Weller M (2003). Hypoxia-induced cell death in human malignant glioma cells: energy deprivation promotes decoupling of mitochondrial cytochrome *c* release from caspase processing and necrotic cell death. *Cell Death Differ* **10**, 823–832.

[13] McClintock DS, Santore MT, Lee VY, Brunelle J, Budinger GR, Zong WX, Thompson CB, Hay N, and Chandel NS (2002). Bcl-2 family members and functional electron transport chain regulate oxygen deprivation-induced cell death. *Mol Cell Biol* **22**, 94–104.

[14] Kroemer G, Galluzzi L, and Brenner C (2007). Mitochondrial membrane permeabilization in cell death. *Physiol Rev* **87**, 99–163.

[15] Kuwana T and Newmeyer DD (2003). Bcl-2–family proteins and the role of mitochondria in apoptosis. *Curr Opin Cell Biol* **15**, 691–699.

[16] Puthalakath H and Strasser A (2002). Keeping killers on a tight leash: transcriptional and post-translational control of the pro-apoptotic activity of BH3-only proteins. *Cell Death Differ* **9**, 505–512.

[17] Nelson DA, Tan TT, Rabson AB, Anderson D, Degenhardt K, and White E (2004). Hypoxia and defective apoptosis drive genomic instability and tumorigenesis. *Genes Dev* **18**, 2095–2107.

[18] Kim JY, Ahn HJ, Ryu JH, Suk K, and Park JH (2004). BH3-only protein Noxa is a mediator of hypoxic cell death induced by hypoxia-inducible factor 1alpha. *J Exp Med* **199**, 113–124.

[19] Bacon AL and Harris AL (2004). Hypoxia-inducible factors and hypoxic cell death in tumour physiology. *Ann Med* **36**, 530–539.

[20] Allalunis-Turner MJ, Franko AJ, and Parliament MB (1999). Modulation of oxygen consumption rate and vascular endothelial growth factor mRNA expression in human malignant glioma cells by hypoxia. *Br J Cancer* **80**, 104–109.

[21] Hetschko H, Voss V, Horn S, Seifert V, Prehn JH, and Kögel D (2008). Pharmacological inhibition of Bcl-2 family members reactivates TRAIL-induced apoptosis in malignant glioma. *J Neurooncol* **86**, 265–272.

[22] Kabeya Y, Mizushima N, Ueno T, Yamamoto A, Kirisako T, Noda T, Kominami E, Ohsumi Y, and Yoshimori T (2000). LC3, a mammalian homologue of yeast Apg8p, is localized in autophagosome membranes after processing. *EMBO J* **19**, 5720–5728.

[23] Kögel D, Svensson B, Copanaki E, Anguissola S, Bonner C, Thurow N, Gudorf D, Hetschko H, Muller T, Peters M, et al. (2006). Induction of transcription factor CEBP homology protein mediates hypoglycaemia-induced necrotic cell death in human neuroblastoma cells. *J Neurochem* **99**, 952–964.

[24] Gozuacik D and Kimchi A (2004). Autophagy as a cell death and tumor suppressor mechanism. *Oncogene* **23**, 2891–2906.

[25] Gozuacik D and Kimchi A (2007). Autophagy and cell death. *Curr Top Dev Biol* **78**, 217–245.

[26] Kondo Y and Kondo S (2006). Autophagy and cancer therapy. *Autophagy* **2**, 85–90.

[27] Kögel D, Reimertz C, Mech P, Poppe M, Frühwald MC, Engemann H, Scheidtmann KH, and Prehn JH (2001). Dlk/ZIP kinase–induced apoptosis in human medulloblastoma cells: requirement of the mitochondrial apoptosis pathway. *Br J Cancer* **85**, 1801–1808.

[28] Mellor HR and Harris AL (2007). The role of the hypoxia-inducible BH3-only proteins BNIP3 and BNIP3L in cancer. *Cancer Metastasis Rev* **26**, 553–566.

[29] Asai A, Miyagi Y, Sugiyama A, Gamanuma M, Hong SH, Takamoto S, Nomura K, Matsutani M, Takakura K, and Kuchino Y (1994). Negative effects of wild-type p53 and s-Myc on cellular growth and tumorigenicity of glioma cells. Implication of the tumor suppressor genes for gene therapy. *J Neurooncol* **19**, 259–268.

[30] Jiang Z, Zheng X, and Rich KM (2003). Down-regulation of Bcl-2 and Bcl-xL expression with bispecific antisense treatment in glioblastoma cell lines induce cell death. *J Neurochem* **84**, 273–281.

[31] Burton TR, Henson ES, Baijal P, Eisenstat DD, and Gibson SB (2006). The pro–cell death Bcl-2 family member, BNIP3, is localized to the nucleus of human glial cells: implications for glioblastoma multiforme tumor cell survival under hypoxia. *Int J Cancer* **118**, 1660–1669.

[32] Degterev A, Lugovskoy A, Cardone M, Mulley B, Wagner G, Mitchison T, and Yuan J (2001). Identification of small-molecule inhibitors of interaction between the BH3 domain and Bcl-xL. *Nat Cell Biol* **3**, 173–182.

[33] Feng WY, Liu FT, Patwari Y, Agrawal SG, Newland AC, and Jia L (2003). BH3-domain mimetic compound BH3I-2′ induces rapid damage to the inner mitochondrial membrane prior to the cytochrome *c* release from mitochondria. *Br J Haematol* **121**, 332–340.

[34] Wang JL, Liu D, Zhang ZJ, Shan S, Han X, Srinivasula SM, Croce CM, Alnemri ES, and Huang Z (2000). Structure-based discovery of an organic compound that binds Bcl-2 protein and induces apoptosis of tumor cells. *Proc Natl Acad Sci USA* **97**, 7124–7129.

[35] Rampling R, Cruickshank G, Lewis AD, Fitzsimmons SA, and Workman P (1994). Direct measurement of pO_2 distribution and bioreductive enzymes in human malignant brain tumors. *Int J Radiat Oncol Biol Phys* **29**, 427–431.

[36] Evans SM, Judy KD, Dunphy I, Jenkins WT, Hwang WT, Nelson PT, Lustig RA, Jenkins K, Magarelli DP, Hahn SM, et al. (2004). Hypoxia is important in the biology and aggression of human glial brain tumors. *Clin Cancer Res* **10**, 8177–8184.

[37] Jensen RL (2006). Hypoxia in the tumorigenesis of gliomas and as a potential target for therapeutic measures. *Neurosurg Focus* **20**, E24.

[38] Graeber TG, Osmanian C, Jacks T, Housman DE, Koch CJ, Lowe SW, and Giaccia AJ (1996). Hypoxia-mediated selection of cells with diminished apoptotic potential in solid tumours. *Nature* **379**, 88–91.

[39] Weinmann M, Belka C, Guner D, Goecke B, Muller I, Bamberg M, and Jendrossek V (2005). Array-based comparative gene expression analysis of tumor cells with increased apoptosis resistance after hypoxic selection. *Oncogene* **24**, 5914–5922.

[40] Weinmann M, Jendrossek V, Guner D, Goecke B, and Belka C (2004). Cyclic exposure to hypoxia and reoxygenation selects for tumor cells with defects in mitochondrial apoptotic pathways. *FASEB J* **18**, 1906–1908.

[41] Steinbach JP and Weller M (2004). Apoptosis in gliomas: molecular mechanisms and therapeutic implications. *J Neurooncol* **70**, 247–256.

[42] Saeki K, Yuo A, Okuma E, Yazaki Y, Susin SA, Kroemer G, and Takaku F (2000). Bcl-2 down-regulation causes autophagy in a caspase-independent manner in human leukemic HL60 cells. *Cell Death Differ* **7**, 1263–1269.

[43] Pattingre S, Tassa A, Qu X, Garuti R, Liang XH, Mizushima N, Packer M, Schneider MD, and Levine B (2005). Bcl-2 antiapoptotic proteins inhibit Beclin 1–dependent autophagy. *Cell* **122**, 927–939.

[44] Pattingre S and Levine B (2006). Bcl-2 inhibition of autophagy: a new route to cancer? *Cancer Res* **66**, 2885–2888.

[45] Shimizu S, Kanaseki T, Mizushima N, Mizuta T, Arakawa-Kobayashi S, Thompson CB, and Tsujimoto Y (2004). Role of Bcl-2 family proteins in a non-apoptotic programmed cell death dependent on autophagy genes. *Nat Cell Biol* **6**, 1221–1228.

[46] Oberstein A, Jeffrey PD, and Shi Y (2007). Crystal structure of the Bcl-xL–Beclin 1 peptide complex: Beclin 1 is a novel BH3-only protein. *J Biol Chem* **282**, 13123–13132.

[47] Maiuri MC, Le Toumelin G, Criollo A, Rain JC, Gautier F, Juin P, Tasdemir E, Pierron G, Troulinaki K, Tavernarakis N, et al. (2007). Functional and physical interaction between Bcl-X(L) and a BH3-like domain in Beclin-1. *EMBO J* (Epub 2007 Apr 19).

[48] Elmore SP, Qian T, Grissom SF, and Lemasters JJ (2001). The mitochondrial permeability transition initiates autophagy in rat hepatocytes. *FASEB J* **15**, 2286–2287.

[49] Bogler O and Weller M (2002). Apoptosis in gliomas, and its role in their current and future treatment. *Front Biosci* **7**, e339–e353.

[50] Kanzawa T, Germano IM, Komata T, Ito H, Kondo Y, and Kondo S (2004). Role of autophagy in temozolomide-induced cytotoxicity for malignant glioma cells. *Cell Death Differ* **11**, 448–457.

[51] Moretti L, Attia A, Kim KW, and Lu B (2007). Crosstalk between Bak/Bax and mTOR signaling regulates radiation-induced autophagy. *Autophagy* **3**, 142–144.